scientific reports

Check for updates

OPEN

Pigment granule architecture varies across yellow, red, and brown chromatophores in squid *Doryteuthis pealeii*

Duncan Q. Bower[1], Stephen L. Senft[2], Roger T. Hanlon[2] & Leila F. Deravi[1]✉

Cephalopods produce dynamic colors and skin patterns for communication and camouflage via stratified networks of neuronally actuated yellow, red, and brown chromatophore organs, each filled with thousands of pigment granules. While compositional analysis of chromatophore granules in *Doryteuthis pealeii* reveals the pigments as ommochromes, the ultrastructural features of the granules and their effects on bulk coloration have not been explored. To investigate this, we isolated granules from specific colored chromatophores and imaged them using multiple modalities. The brown granules are largest with smooth surface coatings. Red granules are intermediate in size with irregular surface textures, and yellow granules are smallest, with rough, porous surfaces. Many of the granules contain sub-granular features that also vary in presentation with color. Correlated light and electron microscopy reveal that differences in hue of individual granules are similarly associated with size, shape, and texture, suggesting that granules may be structurally adapted to modify the dominant visible colors presented within the chromatophores. These findings suggest that granule ultrastructure, not just chemical composition, may be significant in producing the range of colors presented in cephalopod chromatophores.

There are innumerable examples of color production and manipulation in the animal kingdom, yet none are as dynamic, diverse, and sophisticated as that of cephalopods, who have evolved rapid and adaptive modes of color modulation across their bodies for a wide range of communication[1,2] and concealment[3,4]. These vital functions are enabled by thousands of stratified pigmented dermal chromatophore organs in shades of yellow, red, and brown (and, in some taxa, black)[2,5,6], that are layered directly beneath the epidermis in both benthic and pelagic cephalopods[7]. Additionally, a deeper zone of dermis contains a variety of iridophore cell types able to produce a broad range of additional colors through complementary structural (i.e., non-pigmentary) modes of light interaction[8].

Cephalopod chromatophores are dynamic multicellular organs, and structurally distinct from the well-documented chromatophores in some vertebrate species[9,10]. Their central and largest cell, the chromatocyte, contains pigmented material within a highly flexible sacculus. Attached around the perimeter of the chromatocyte are several dozen highly innervated radial muscle cells, innervated monosynaptically from the central nervous system[3,6,11], that undergo rapid cycles of contraction and relaxation (ca. 200 ms in duration[12]). These periodically reshape the chromatocyte into a nearly flat disc with presented surface areas up to 14 times that of its relaxed spheroidal punctate (retracted) state[5]. The terminating axonal processes are surrounded by glial cells that provide functional insulation and perhaps also structural and metabolic support. Likewise, the chromatocyte and the directly interfacing muscles are entirely encapsulated by numerous smaller highly folded "sheath" cells, whose function is not understood but is presumed to provide a low-viscosity spatial domain within which the chromatophores can actuate[6,13,14].

The pigmentation of chromatophores is provided by ommochromes, including xanthommatin and decarboxylated xanthommatin, residing within ommochromasomes (commonly called pigment granules) that fully populate each chromatocyte sacculus[7,15–18]. This class of molecules appear in a range of visible colors, due to an ability to undergo redox-based color change (reflecting and transmitting yellows in the oxidized state, reds in the reduced state, and browns when at high concentrations)[19]. Although too slow to be employed in the animal's rapid adaptive camouflaging capabilities, the redox-dependent coloration is efficient developmentally, allowing one type of compound to be packaged and sequestered as three canonical colors (yellow, red, or brown), possibly

[1]Department of Chemistry and Chemical Biology, Northeastern University, Boston, MA 02115, USA. [2]Marine Biological Laboratory, Woods Hole, MA 02543, USA. ✉email: l.deravi@northeastern.edu

in ontogenic temporal sequence[16]. However, little information exists regarding the physical parameters (e.g.: size, density, geometry) of the resulting granules and how they may impact these ontogenetic optical processes.

The development and maturation of chromatophores have been studied in the cuttlefish *Sepia officinalis*. Their colors develop systematically, beginning as pale yellow and changing to red and ultimately brown over a span of 25 days, starting with seven-day-old hatchlings[16]. Similar pigmentary progressions have been noted in *Octopus vulgaris*, in which the age of chromatophores correlates directly with both size and color, with darker colors developing later in the lifespan of a chromatophore[20]. However, these observations are case studies of holistic chromatophore maturation and do not describe changes at the level of granule structure and density. In fact, the origins of the pigment granules remain largely unknown across cephalopod biology, although it has been proposed that the granules are lysosome-related organelles like those found in crab spiders[17,21]. It remains unclear where or when the granules originate and by what mechanisms they become specialized to produce variety in the visible coloration system across cephalopod skin.

In this report, we isolate and analyze granules extracted from yellow, red, and brown chromatocytes from the longfin squid *D. pealeii* employing several methods. Using light and electron microscopy, we uncover correlations of transmitted and reflected color with granule surface nanostructure and with internal electron density. Individual granules vary in optical hue, a feature that covaries with morphological subtype. Combining our findings with prior studies of cephalopod coloration, we propose a connection among chromatophore pigment color, granule structure, and biochemistry, and we highlight key questions that can lead to new classes of bio-inspired color-rich materials.

Methods

Sourcing and treatment of squid specimens

D. pealeii were obtained from the Marine Biological Laboratory in Woods Hole, MA. When possible, fresh samples were used; otherwise, specimens that had been frozen when fresh were subjected to minimal freeze-thaw cycles before analysis. Care was taken to minimize the number of animals used. For fresh samples, live specimens were anesthetized in ethanol before sacrifice[22].

Preparation of granule samples through enzymatic digestion and washing

Once the specimen was terminally anesthetized, the epidermal layer of skin was removed. The chromatophore layer was dissected from the iridophore layer below before being placed in a solution of 6 mg/mL collagenase (*C. histolyticum*, Sigma-Aldrich) in filtered sea water, similarly to previous reports[23]. This solution was incubated at 4 °C for several days with regular gentle trituration to break up the collagen-rich extra-cellular matrix surrounding the chromatophores. The solution was replaced daily to mitigate microbial growth.

After chromatophores were liberated from the extra-cellular matrix, they were manually isolated into distinct color populations with a micropipette tip with the aid of a Nikon SMZ18 stereo microscope and placed onto square glass cover slips (Coverglass No. 1, 25×25 mm, Fisherbrand). They were then carefully washed using capillary tubes several times, inducing destruction of the outer surface of the chromatophore saccule and diffuse dispersal of the granules across the surface of the cover slip. For SEM, these samples were air-dried and further prepared by mounting the cover slips on SEM pin stubs using carbon adhesive tape and graphite paste to promote conductivity. Then the samples were sputter-coated with 2.5 nm gold/palladium (108auto, Cressington).

Preparation of granule samples using fixative

Whole chromatophores from freshly excised squid dermis were treated with Hollande's fixative, embedded in paraffin, sectioned to a thickness of 6 µm, and dry-mounted on slides. The sections were deparaffinized and sputter-coated with 9 nm platinum. Photomicrographs of the coated sections were also taken to estimate the original optical transmission color of the chromatophores.

Light microscopy of granules

Light microscopy was performed using an upright Zeiss Axiozoom V16 (Maximum magnification and WD: 5.6X/10 cm; 25X/1 cm) or IM35. These images were used to verify chromatophore purity and confirm the visible color of the isolated chromatophores on the cover slip, as well as correlate them to those species imaged on the SEM.

Scanning electron microscopy (SEM) of granules

SEM of granules was performed using either a Zeiss Supra 25 SEM or a Zeiss Supra-V40 SEM. Images were taken in secondary electron or in-lens modes using accelerating voltages of 3.0–7.0 kV.

Measuring the average size and morphology of different granule populations using FIJI

SEM images were processed and analyzed using FIJI[21]. The elliptical selection tool was used to manually trace each particle in the images of the various color populations. These were saved as regions of interest and the major and minor axes of each particle were calculated based on the scale of the image. Roughly 9000 granules from 20 SEM images were measured in this way, from 24 chromatophores derived from approximately ten *D. pealeii* specimens.

Serial block-face imaging (SBFI)

Dorsal mantle from an anesthetized adult *Doryteuthis pealeii* squid was excised and immersed in Karnovsy's fixative and processed through osmium and into Epon according to a modified Ellisman OTO protocol[24]. Trimmed blocks containing chromatophore organs was sent to FEI Inc. who generated 3D serial block face

SEM data imaged at 10 × 10 × 60 nm using their Teneo system, additional blocks were sent to Gatan, Inc [13.9 × 13.9 × 25 nm, or 65 nm isotropic], and ConnectomX, Inc [16 × 16 × 25 nm, Katana system].

Preparation and imaging of whole-cell single color populations using transmission electron microscopy (TEM)

Chromatophore populations of each color ($n \sim 50$) were enzymatically isolated as described above and immediately placed in a fixative containing 3% glutaraldehyde, 0.1 M sodium cacodylate buffer (pH 7.4), and 0.35 M sucrose to control osmotic pressure. After overnight incubation in the fixative at 4 °C, the cells were centrifuged (5000 g, 10 min) and the fixative was removed by soaking 3x with 0.1 M sodium cacodylate buffer (pH 7.4, with sucrose) for 10 min each. Osmium tetroxide at a concentration of 1% (m/v) in sodium cacodylate buffer was then added for a one-hour incubation time. Following staining with osmium tetroxide, the sample pellets were washed again with 0.1 M sodium cacodylate buffer 3x for 10 min each. The buffer was then progressively exchanged with a series of ethanol/water solutions to effectively dry the samples, until the samples were contained in 100% ethanol. A hybrid epoxy resin was prepared with the following recipe, listed here with associated mass percents: Quetol 651 (12.0% m/m), ERL 4221 (19.1% m/m), nonenyl succinic anhydride (54.9% m/m), DER 736 (12.3% m/m), and BDMA (1.7% m/m). All resin ingredients were sourced from Electron Microscopy Sciences. Certain samples were instead processed using Karnovsky fixative for one hour. The samples were then osmicated and progressively exchanged to the hybrid resin mixture or to Epon, transferred to block capsules, and incubated at 60 °C to induce polymerization. When the blocks were solid, they were removed from the capsules and trimmed and sectioned. Thin sections (thickness ~ 80 nm) were cut using an ultramicrotome (Reichert Jung Ultracut E) equipped with a diamond-tipped sectioning knife and placed on TEM grids for imaging. Images of the thin-sectioned materials were taken using a transmission electron microscope (JEOL JEM 1010). An accelerating voltage of 60 kV was used.

Results

Chromatophores in *D. pealeii* present as interlocking discoid units (Fig. 1a)[5] comprising three canonical colors: a central dark brown (here in the punctate state), encircled by quasi-alternating reds and lighter browns, themselves interspersed with smaller yellow chromatophores (Fig. 1b). Images collected from the different actuation states (punctate versus expanded) of part of a discoid unit from intact skin reveal an uneven distribution of reflected colorant with the densest color observed in the center (Fig. 1c). Unevenness in coloration is also visible using transmitted light microscopy on excised chromatophore tissue (Fig. 1d). Interestingly, the coloration remains markedly uniform in a wide peripheral zone of each expanded sacculus, suggesting that granules are connected with near neighbors (loosely, since linkages in the third dimension are clearly labile). Transverse sections of expanded chromatophores suggest that the layers of granules decrease from 3 or more granule layers thick to 2 granule layers thick towards the outer extremity of the saccule (Fig. 1d, inset). These observations indicate regional differences in location and translocation of the granules that may contribute to slight differences in color within one chromatophore.

Closer examination of optical images of isolated and washed chromatophores exposed several noteworthy relationships between granules and the chromatophores they inhabit. First, to the extent that the individual color of granules could be resolved using light microscopy, the color of a given granule is not fully dictated by the color of the chromatophore it inhabits. For instance, while a canonically brown chromatophore is made up predominantly of visibly brown granules, interspersed red and yellow granules are also observed using reflected light microscopy (Fig. 1e). Similarly, some reflective yellow colors can be seen in a canonically red chromatophore (Fig. 1f). These indicate that a specific chromatophore's color (which can vary subtly from the canonical groupings, see Fig. 1b, c) might be the result of contributions from multiple types of granules.

When groups of pigment granules from different chromatophore colors were combined and imaged using both light microscopy and SEM, it was directly apparent that granule size, morphology, and color are correlated and that each canonical color has a unique granule profile (Fig. 2a, b). Specifically, visibly brown granules appear smoother and rounded, whereas yellow and red granules are noticeably smaller and more textured, respectively (Fig. 2c). These observations suggest that visible color correlates to the intrinsic anatomical properties of the granules themselves. Moreover, no single granule was observed exhibiting multiple colors or morphology associated with multiple colors. In principle, this could have been due to limited resolution; however, granules close enough to touch each other showed different hues with visible differences in sizes and/or textures. Hence, it appears that each granule presents its own color profile.

To determine whether granule size is the differentiating factor across the differently colored chromatophores, we measured the diameters of granules enzymatically derived from brown, red, and yellow chromatophores and imaged via SEM as 461 ± 96 nm ($n = 5002$), 391 ± 69 nm ($n = 1005$), and 369 ± 86 nm ($n = 2429$), respectively (Fig. 2d). A one-tailed t test revealed that the yellow granules were significantly smaller than both the red and brown granules ($p < 0.0001$), and the red granules were significantly smaller than the brown granules ($p < 0.0001$) (Fig. 2e). Given these subtle, but significant, differences in the diameters, we investigated how changes to the sample preparation may have impacted these findings. All initial analysis was conducted using unfixed granules from saccules that had been sorted manually and rinsed briefly with distilled water before sputter coating and imaging with SEM (Fig. 3a). We compared these samples against granules subjected to Hollande's fixative, paraffin embedding, sectioning, deparaffinization, and sputter coating (Fig. 3b). In the enzymatically liberated and water-washed samples, yellow granules consistently appeared spherical or ellipsoidal with subtle, nanotextured surface deformations or sub-granular structures (Fig. 3a.i.). Red granules, in contrast, were most frequently observed to be visibly mottled with a wrinkled texture (Fig. 3aii). Brown granules were the most distinctly coherent of the three populations, with a smooth surface texture and clearly delineated granule boundaries (Fig. 3aiii). By contrast, in fixed yellow samples (Fig. 3bi), granules were observed as smaller (mean diameter 293 ± 54, $n = 125$),

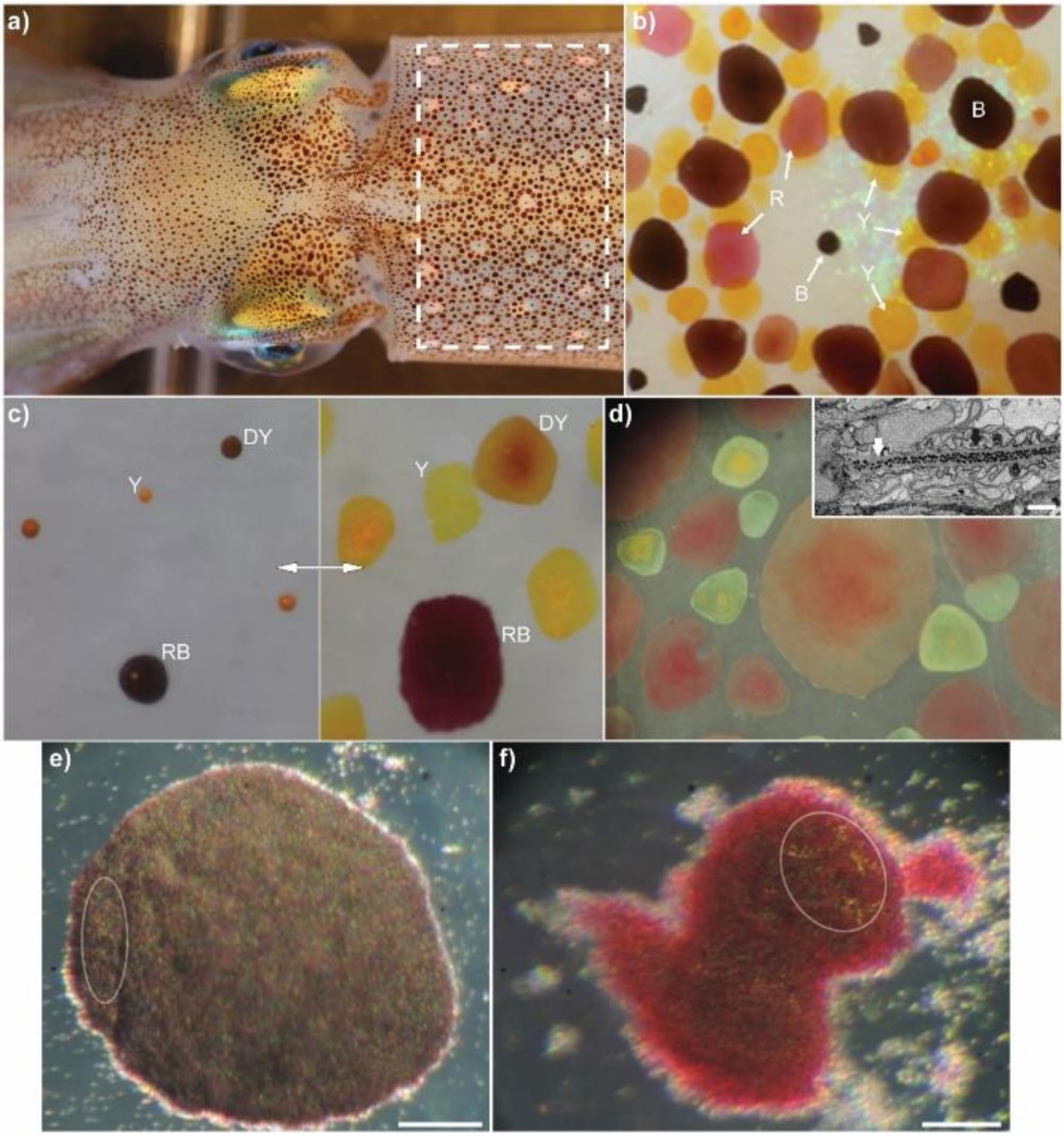

Fig. 1. Variations in chromatophore colors in squid *D. pealeii* chromatophores. (**a**) The color display of an adult *D. pealeii* with the dorsal area highlighted (roughly 25 cm^2). (**b**) A discoid unit of the squid chromatophore as rendered in its expanded form, with the central brown saccule held punctate. Canonical colors are indicated: Y = yellow, R = red, B = brown. Based on the documented size of discoid units[5], the approximate size of the figure is roughly 20 mm^2. (**c**) Chromatophores in their retracted and expanded states: Y = yellow, DY = dark yellow, RB = red-brown. Images are roughly 2 mm^2 in area. (**d**) Transmitted-light microscopy image highlighting color density is highest at the center of the chromatophores, suggesting a differential distribution of granules. Image is roughly 6 mm^2 in area. Inset is TEM image of transverse cross-section of expanded chromatophore, supporting this observation. Granules are stained dark with osmium and are visibly less densely distributed at the edge of the saccule (white arrow) than nearer the center (black arrow). Scale bar is 5 μm. (**e**,**f**) Enzymatically liberated brown and red chromatophores under stereoscope demonstrate a diversity of "micro-colors" presented in one chromatophore. Variance can be seen throughout the chromatophore, but areas of high color diversity are indicated with ellipses. Scale bars are 50 μm.

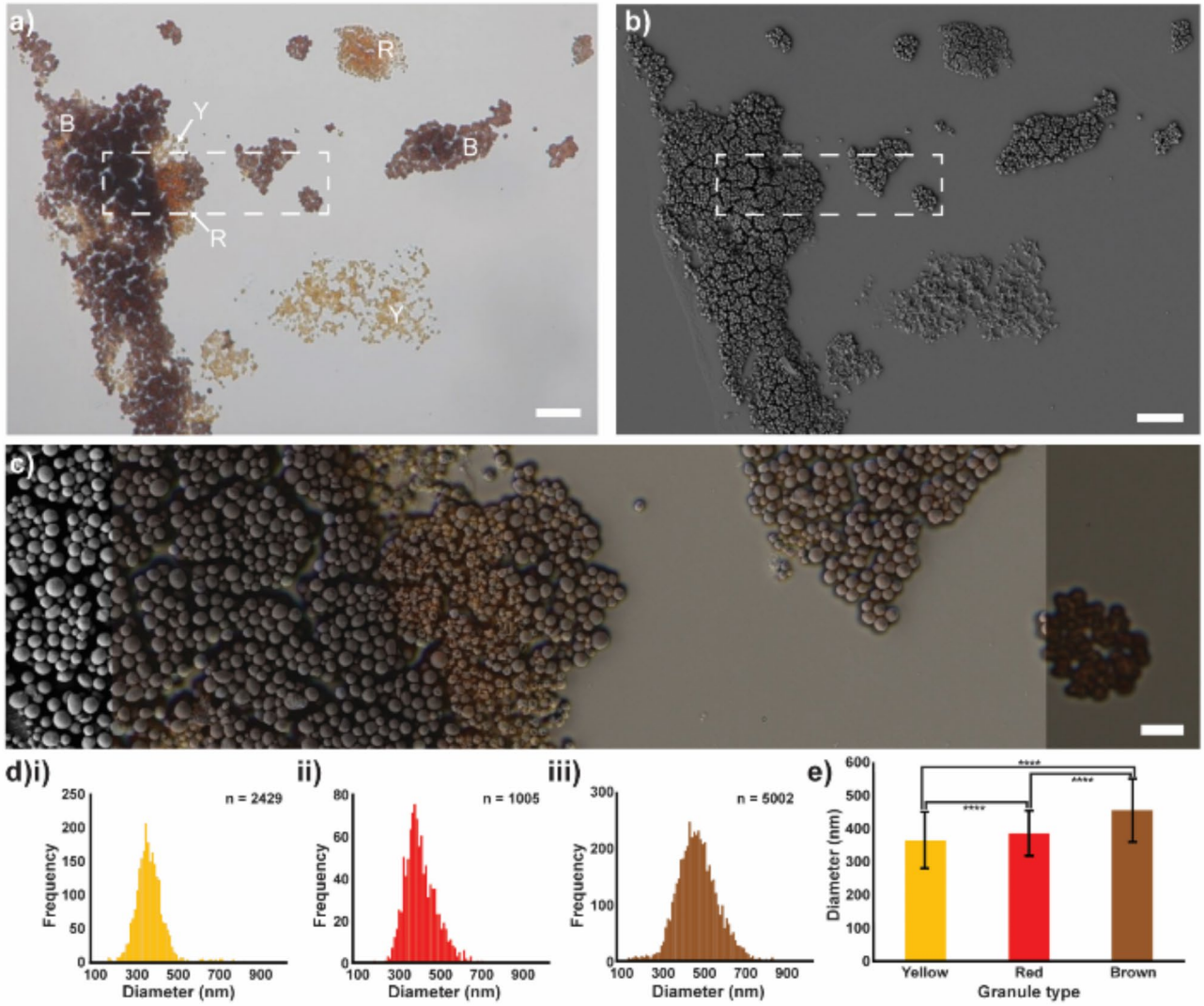

Fig. 2. Size, morphology, and color of chromatophore granules are correlated. (**a**) Light microscope image of different enzyme-liberated chromatophores shows that granules themselves have distinct color. Y = yellow, R = red, B = brown. Scale bar is 10 µm. (**b**) SEM image of the same sample, allowing for granule-level resolution of size and texture. Scale bar is 10 µm. (**c**) A coordinated overlay of the region of interest marked by dashed rectangle in (**a**) and (**b**) clearly demonstrates difference in texture and size of granules between regions of different colors. Scale bar is 2 µm. (**d**) Size distribution histograms of the measured diameters of granule populations. (**e**) Size comparison of the mean diameters of the three canonical color populations. All population means were significantly different from one another using a one-tailed t-test ($p < 0.0001$).

textured particles. Red granules (Fig. 3bii) were similarly textured and deformed as in washed samples but, again, observed with a smaller mean diameter (384 ± 58, $n = 69$). Interestingly, the brown granules (Fig. 3biii) appeared 21% larger than the unfixed, water-washed samples (mean diameter 558 ± 95 nm. $n = 625$). While the trends remained the same (yellow < red < brown granules), our findings suggest that post-processing methods may have had an impact on granule size and structure.

Given these differences, we asked whether it would be possible, in a third mode of tissue preparation, to assign a color categorization based on the size of granules alone. To test this, we analyzed granule sizes from a fixed chromatophore using serial block face imaging (SBFI). By scanning through multiple frames of a z-stack with 60 nm spacing, we recorded an average granule size of 561 ± 126 nm (Fig. 4a, $n = 379$). It was difficult to assign a color value to these granules based on size, although the measured diameters suggest a bimodal distribution with peaks at ~480 nm to ~680 nm, strongly suggesting a red-brown colored chromatophore. In a separate volumetric image of another large chromatophore (also of uncertain color), we performed the same z-stack analysis (752 ± 188 nm, Fig. 4b, $n = 64$). Since these values surpass the others collected from the isolated and processed granules, they strongly suggest that these granules are large brown types. While these findings could not be validated, as the origin of color from this sample was unknown, our data reveal applications of our

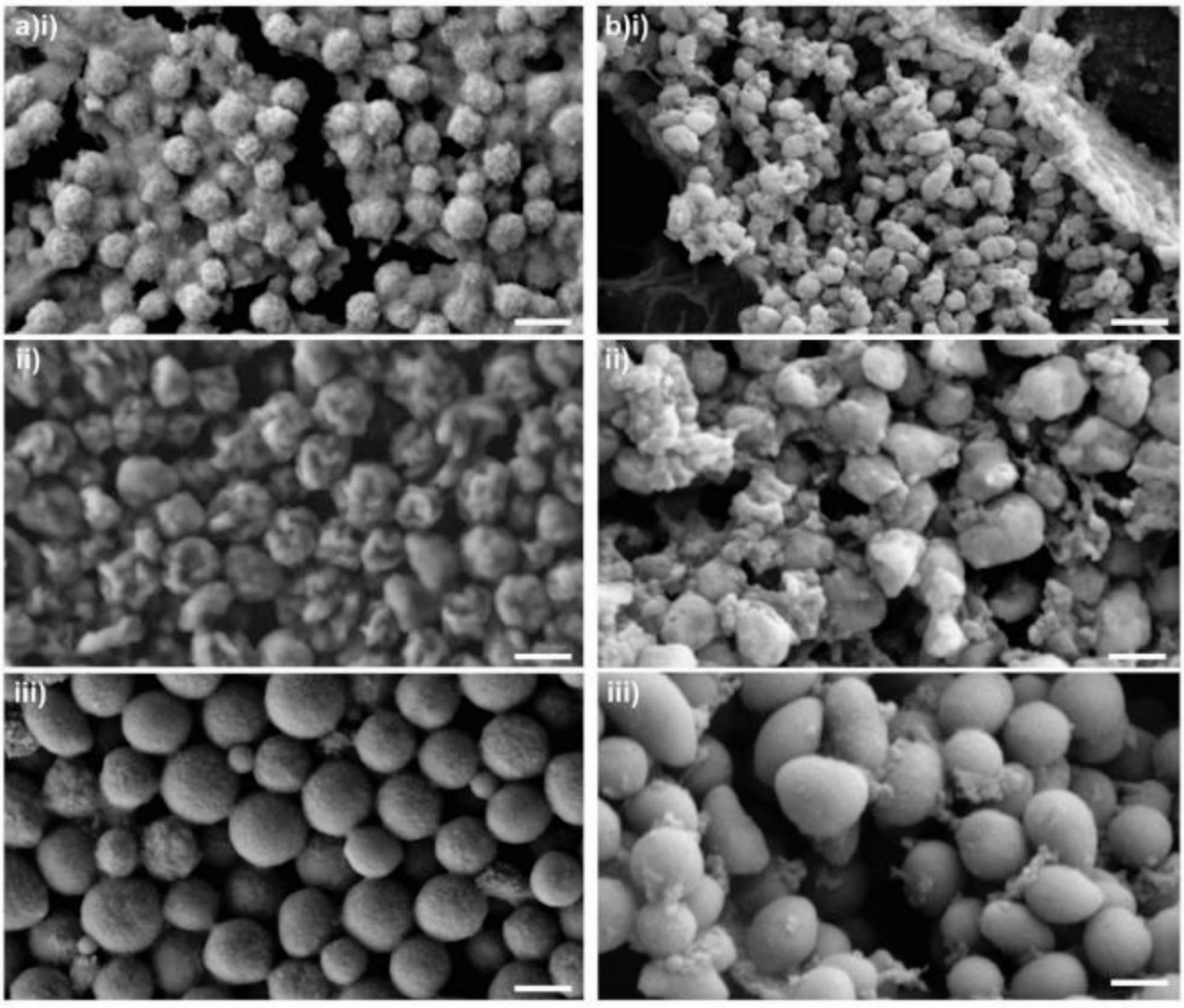

Fig. 3. SEM images demonstrate differences in size and morphology between pigment granules from yellow, red, and brown chromatophores. All scale bars are 500 nm. (**a**) Water-washed and isolated granules from (i) yellow, (ii) red, and (iii) brown granules. (**b**) Granules prepared with Hollande's fixative, where (i) yellow, (ii) red, and (iii) brown granules appear differently in surface texture than enzyme-treated, water-washed samples.

size-based classifications using an orthogonal imaging technique that provides indirect evidence of the color state.

In the SBFI images, we observed different gradients in the local electron densities of the granules (Fig. 4a, b). To further explore these variations, we expanded our analysis to TEM (fixed similarly to the SBFI tissue) to provide insight as to the internal osmiophilicity of the granules. Because all three populations were treated with the same degree of osmium tetroxide staining, osmiophilicity can be used as a guide with which to distinguish the internal structure of the color populations, since a structure's affinity for osmium is directly proportional to its electrophilicity in the observed TEM micrographs. The most uniform of the three populations was the yellow granule set, which demonstrated a high degree of consistency in the osmiophilicity across single granules. In contrast, the red and brown granule populations had notable variation in osmiophilicity, both between granules and across individual granules, suggesting both a diversity of morphological development and differentiation within these granule subtypes that varied between granules isolated from red and brown colors (Fig. 4c, d). In some samples of red granules, the section passed through the observed central core of the granule, revealing a gap in the center of the structure. (Fig. 4dii).

Irrespective of preparative mode, another trend across granules of different canonical colors was their interstitial matrix. In brown samples, there was very little material between the large, smooth granules. Moving from brown to red to yellow, however, there was an observable increase in interstitial material that appeared as small flakes surrounding red granules (Fig. 3bii) and as film surrounding granules from yellow chromatophores (Fig. 3ai, bi). Because this film was not observed in red or brown chromatophores (but was consistent across both preparatory conditions), we asked whether it may be a marker for granule development, where yellow

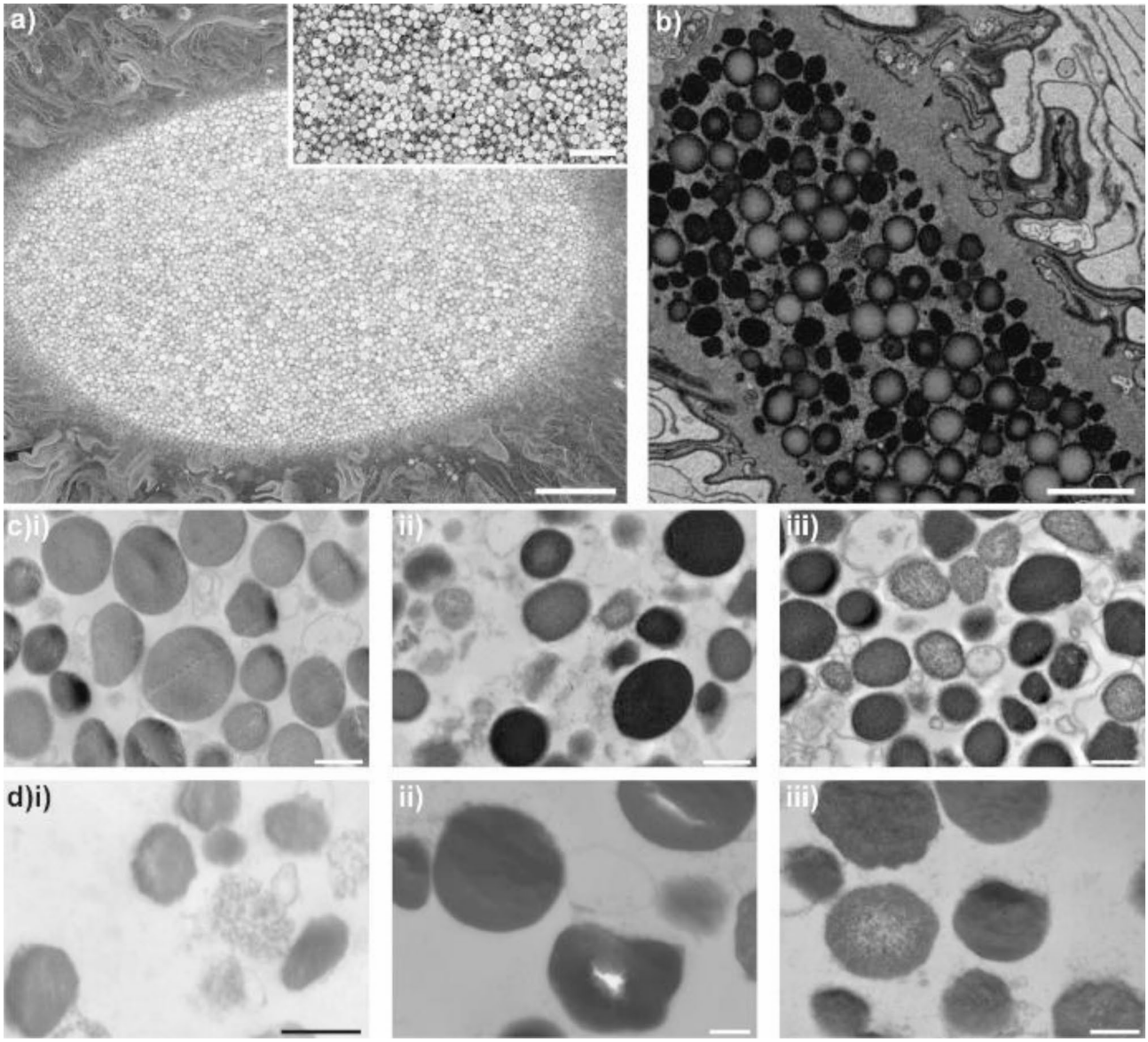

Fig. 4. Sectioned granule samples imaged using SEM and TEM. (**a**) SBFI-SEM imaging of an epoxy-embedded whole-tissue sample. Full-region imaging shows the high packing density of a punctate, undigested chromatophore (color unknown). Scale bar is 10 μm. Insert is a contrast-enhanced detail of granules from same sample. Scale bar is 2 μm. (**b**) A single slice of a z-stack used to measure the three-dimensional size of granules. Scale bar is 2 μm. (**c**) TEM micrographs of color-isolated samples. i) Yellow granules are the least osmiophilic subset, with very little variation in electron density. ii), iii) Red and brown granules, respectively, have more variety in granule osmiophilicity. Scale bars in e are 500 nm). (**d**) A separately processed batch of granules of (i) yellow, (ii) red, and (iii) brown granules. Scale bars in d are 250 nm.

chromatophores may be present as the least matured granule type. Thus, we imaged granules with SEM from a washed yellow-orange chromatophore derived enzymatically from a hatchling squid (Fig. 5a). Qualitatively, these hatchling granules appeared similar to those of adult yellow chromatophores, although with a marked increase in the proportion of granules with ellipsoidal morphology relative to spheres. They are also slightly larger than adult yellow granules, with an average diameter of 426 ± 108 nm ($n = 106$). Because all the embryonic chromatophores that happened to be imaged appeared yellow-orange in color, we could not extend these comparisons to other colored chromatophores.

In adults, we noticed other variations in subsets of red granules (both those from red chromatophores, and in isolated granules that appeared optically red) when water-washed for SEM imaging. Certain red granules have large hollow cavities at their center (Fig. 5b), further supporting our TEM observations (Fig. 4dii). While occasional defects in the granule surface were considered artifacts of the imaging preparation process, the fact that these cavities were only observed in canonically red granules suggested either that the internal material of red granules may be particularly water-soluble or that the surface of the red granules is uniquely prone to

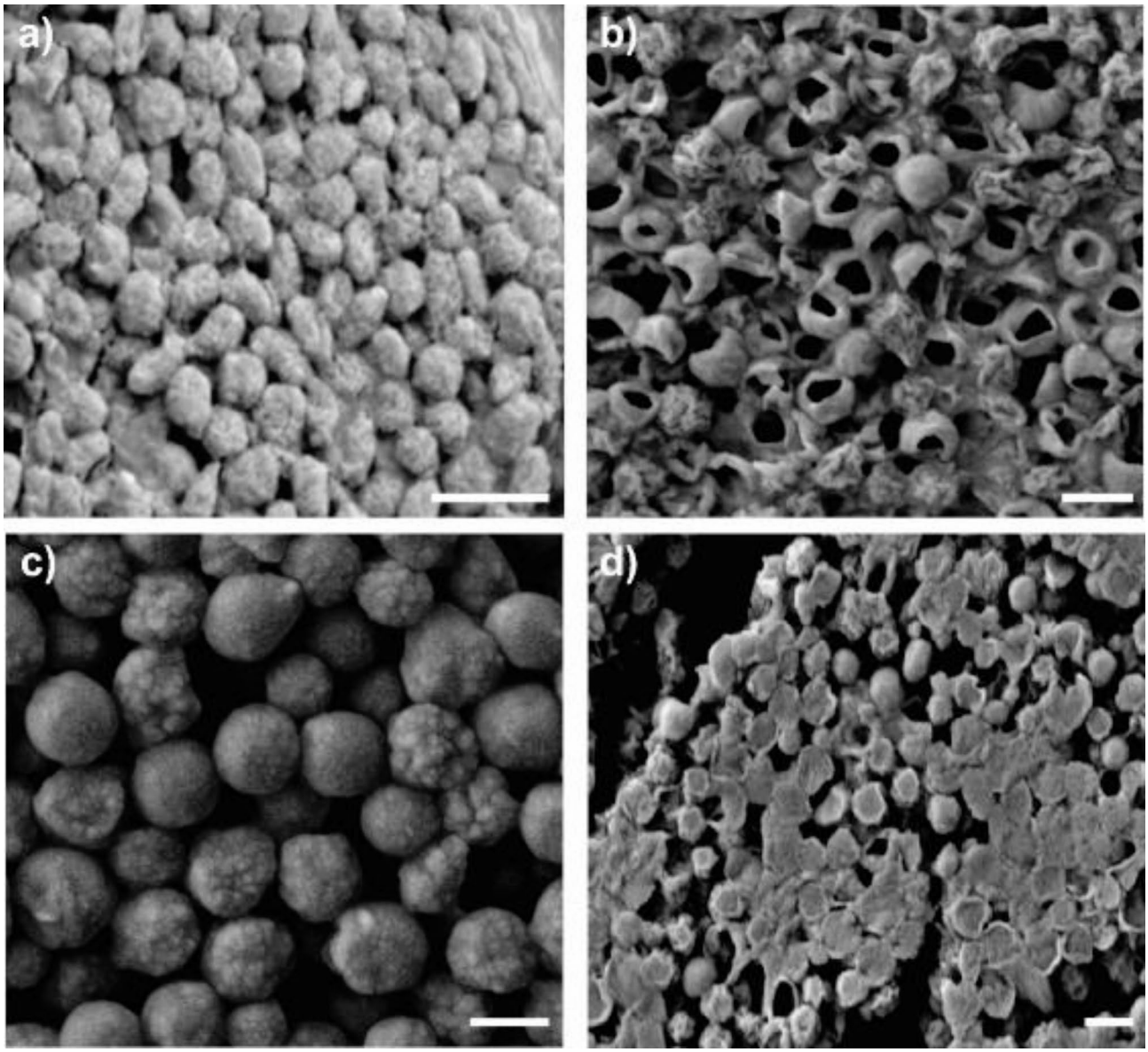

Fig. 5. SEM images of additional populations of granules. (**a**) Fixed granules from hatchling chromatophores (yellow-orange). (**b**) An imaging artifact of some adult-derived red granules reveals certain red granules have hollow cores, which might be revealed with water wash of soluble contents. This also may explain the apparent deformation of other red granules, as the hollow core of the granules may not sustain the pressures of sample preparation. (**c**) A sample of granules from an adult light brown chromatophore suggests a transitional state between yellow and red canonical colors, in which the visible substructures of yellow granules become larger, eventually distorting the overall granule shape. (**d**) Granules of unknown color type, deformed with a coverslip, reveal their malleability and a distinction between the internal contents and their boundary membranes. Scale bars are 500 nm.

deformation. When we isolated granules from intermediate colored light brown or red-brown chromatophores, we observed interesting mixtures of granule subtypes. Some granule populations exhibit smooth surfaces, as observed in Fig. 2; however, some show sub-granular composition similar to those found in the yellow sub-type, albeit with larger sub-granular particles (87 ± 25 nm, $n = 65$; Fig. 5c). The latter were more obvious after contrast-enhancement. Variations in tissue processing conditions also revealed details of granule composition. In one case, a sample of an unrecorded color type was intentionally compressed after it was processed via enzymatic and water-washed treatments and mounted on a coverslip. SEM imaging of the resultant, dried product showed that granules were deformed by the manual compression, suggesting a clay-like consistency and with visible granule coating (thicknesses ranging from 20 to 40 nm, $n = 30$; Fig. 5d), suggestive of the canonical brown granules.

Discussion

It is well-known that composition and structure potentiate color in nature[25,26]. The color created by a biological system is often much more vibrant than the sum of its parts, and precise arrangements of molecules like melanin, guanine, pterin, or isoxanthopterin can yield brilliant blues in birds[27,28], provide complete access to the visible spectrum in chameleons[29], create bright color displays in butterflies and damselflies[30–32], or make up the tunable reflective tapeta of the prawn[33], respectively. However, this potential for structural coloration has not been explored in detail for cephalopod chromatophores. Compositional contributions to the canonical red, yellow, and brown (concentrated yellow) colored chromatophores have been attributed to different oxidation states of ommochrome pigments[34–36]. However, the size and shape of a granule (also providing more concentration of pigment) potentially also govern the granule's ability to produce structural color and/or increase optical density, where the pathlength of light will increase proportionally with particle diameter. The granule structure itself may also serve a protective function—shielding the pigment against auto-oxidation or photobleaching through confinement[37]. Recent transcriptomic investigation of the pigment granules has revealed an abundance of specialized crystallin proteins, which may coordinate with ommochromes to reduce oxidative stress[13]. It is possible that granule ultrastructure becomes modified by this binding relationship, as the variously reduced ommochrome-crystallin complexes (along with auxiliary proteins) are propagated throughout the granule structures during ontogeny. Despite these speculations in function, it is currently unclear why granules are present with unique colors, textures, sizes, and shapes that are sequestered to different chromatophore types.

Ommochrome granules have been identified in a number of arthropods and cephalopods for crypsis and mimicry (such as in the epidermis of the squid or crab spider) or for signaling and maturation (as in the ommatidia of the dragonfly or fruit fly)[38–43]. In various Odonata, pigment granules and pigmentary vesicles sourced from the compound eye range from 0.15 to 0.80 μm[42]. In wild type *Drosophila melanogaster*, ommochrome granules are present with 0.30–0.67 μm diameters in mature specimens, with growth of these particles developing exponentially over time[41]. In a study of dark brown/black pigment granules of both the eye and body of some crustaceans, an average diameter of 0.6 μm is reported[38]. These results are generally in accordance with the observations in the present study, although many of these species do not possess the differential coloration seen in the squid. One exception is the crab spider *Misumena vatia*, which processes ommochrome granules that undergo catabolism and anabolism for color change[43,44]. Insausti and Casas categorized the formation of granules in these animals through three successive steps. In "type I" pro-granules produced from the endoplasmic reticulum, granules are translucent and with diameters ranging from 0.8 to 1.4 μm. A transient "type II" pro-granule emerges next, as type I granules merge to produce larger (1.0–1.6 μm) intermediary diameters with a light-yellow color and notable internal vesicles. Finally, the "type III" granule forms as osmophilic/electron dense, spherical granules with diameters ranging from 0.8 to 1.0 μm[43,44]. While some of these trends are similar to our observations of yellow, red, and brown pigment granules in *D. pealeii*, the *M. vatia* pigment granules are ~2x larger in diameter than squid pigment granules and seemingly do not follow a linear growth sequence. Furthermore, the fully mature type III granules of *M. vatia* are yellow in color. Based on these differences, it seems that the squid has a unique system for developing and distributing its ommochrome granules throughout the different colored chromatophores. Other differences in granule structure are also evident in the variable morphologies of melanosomes in certain birds[45]. In avian melanosomes specifically, there is a unique internal structural degradation following deposition of the organelle in the feather. One explanation for this effect is the introduction of an additional low refractive index material: air[46]. Similar internal processing may also be noted in the *D. pealeii* chromatophore granules, where it is possible that the hollow appearance of red pigment granules may be suggestive of similar defects to elicit optical function.

Regardless of its origin, we noticed several observable trends from yellow to red to brown granules: (1) size increases, (2) the presence of visible interstitial material decreases, and (3) sub-granularity and texture both change (i.e., particles become smoother). When compared to the putative model for ommochromasome formation[17] that likens pre-ommochromasomes, or pre-granules, to endosome derived organelles, the chromatophore granules also present multi-vesicular bodies, or sub-granularity. Thus it is possible that the sub-granular particles noted here, which are most obvious in yellow granules, could be vesicles that have similarly combined to form a pre-granule. Based on our anatomical investigations, we posit that the extra-granular material may deposit or absorb onto the pre-granule surface to smooth out surface textures, increase the overall granule size, and increase the osmophilic/electron density in the granule. This hypothesis provides a starting framework that might be explored further with alternative, advanced imaging modalities such as PFIB SEM[47] to image granules in situ from fixed undigested tissue that also retains visible chromatophore color assignment.

Other future work includes building experimental and computational models of color development and granule maturation, where molecular composition and the nuanced differences in granule ultrastructure are combined. Because the color of the chromatophore is created in large part by ommochrome pigments, redox modification is likely the mechanism for color change from yellow to red[36,48]. Thus, it appears possible that redox-dependent color changes are produced locally within each granule and that each color chromatophore may present more or fewer redox agents to facilitate this process during development, as granules within a given chromatophore can have different color appearances. How the redox process could be synchronized so as to mature populations (or even single granules) uniformly remains under investigation, as we continue to uncover the mysteries surrounding color evolution in these remarkable creatures.

Data availability

Data are provided within the manuscript.

Received: 1 November 2024; Accepted: 10 December 2024

Published online: 28 December 2024

References

1. Wilson, D. J., Lin, Z., Bower, D. Q. & Deravi, L. F. Engineering color, pattern, and texture: from nature to materials. *Matter* **4**(7), 2163–2171 (2021).
2. Hanlon, R. T. & Messenger, J. B. Adaptive coloration in young cuttlefish (*Sepia officinalis* L.): the morphology and development of body patterns and their relation to behaviour. *Phil Trans. R Soc. Lond. B.* **320**, 437–487 (1988).
3. Messenger, J. B. Cephalopod chromatophores: neurobiology and natural history. *Biol. Rev. Camb. Philos. Soc.* **76**(4), 473–528 (2001).
4. Hanlon, R. T. & Messenger, J. B. *Cephalopod Behaviour* (Cambridge University Press, 2018).
5. Hanlon, R. T. The functional organization of chromatophores and iridescent cells in the body patterning of *Loligo plei* (Cephalopoda: Myopsida). *Malacologia* **23**, 89–119 (1982).
6. Florey, E. Ultrastructure and function of cephalopod chromatophores. *Am. Zoologist.* **9**, 429–442 (1969).
7. Dinneen, S. R., Osgood III, R. M., Greenslade, M. E. & Deravi, L. F. Color richness in cephalopod chromatophores originating from high refractive index biomolecules. *J. Phys. Chem. Lett.* **8**(1), 313–317 (2017).
8. Sumathirathne, L., Kim, T., Bower, D. Q. & Deravi, L. F. Cephalopods as a natural sensor-display feedback system inspiring adaptive technologies. *ECS Sens. Plus* **2**(2) (2023).
9. Nilsson Skold, H., Aspengren, S. & Wallin, M. Rapid color change in fish and amphibians - function, regulation, and emerging applications. *Pigment Cell. Melanoma Res.* **26**(1), 29–38 (2013).
10. Aspengren, S., Skold, H. N. & Wallin, M. Different strategies for color change. *Cell. Mol. Life Sci.* **66**(2), 187–191 (2009).
11. Dubas, F., Hanlon, R. T., Ferguson, G. P. & Pinsker, H. M. Localization and stimulation of chromatophore motoneurones in the brain of the squid, *Lolliguncula brevis*. *J. Exp. Biol.* **121**, 1–25 (1986).
12. Hadjisolomou, S. P., El-Haddad, R. W., Kloskowski, K., Chavarga, A. & Abramov, I. Quantifying the speed of chromatophore activity at the single-organ level in response to a visual startle stimulus in living, intact squid. *Front. Physiol.* **12**, 675252 (2021).
13. Williams, T. L. et al. Dynamic pigmentary and structural coloration within cephalopod chromatophore organs. *Nat. Commun.* **10**(1), 1004 (2019).
14. Cloney, R. A. & Brocco, S. L. Chromatophore organs, reflector cells, iridocytes and leucophores in cephalopods. *Amer Zool.* **23**, 581–592 (1983).
15. Crawford, K. et al. Highly efficient knockout of a squid pigmentation gene. *Curr. Biol.* **30**(17), 3484–3490e4 (2020).
16. Reiter, S. et al. Elucidating the control and development of skin patterning in cuttlefish. *Nature* **562**(7727), 361–366 (2018).
17. Figon, F. & Casas, J. Ommochromes in invertebrates: biochemistry and cell biology. *Biol. Rev. Camb. Philos. Soc.* (2018).
18. Deravi, L. F. et al. The structure-function relationships of a natural nanoscale photonic device in cuttlefish chromatophores. *J. R Soc. Interface.* **11**(93), 20130942 (2014).
19. Figon, F., Casas, J., Ciofini, I. & Adamo, C. Electronic coupling in the reduced state lies at the origin of color changes of ommochromes. *Dyes Pigm.* **185**, 108661 (2021).
20. Packard, A. Morphogenesis of chromatophore patterns in cephalopods: are morphological and physiological 'units' the same? *Malacologia* **23**, 193–201 (1982).
21. Figon, F., Deravi, L. F. & Casas, J. Barriers and promises of the developing pigment organelle field. *Integr. Comp. Biol.* **61**(4), 1481–1489 (2021).
22. Abbo, L. A., Himebaugh, N. E., DeMelo, L. M., Hanlon, R. T. & Crook, R. J. Anesthetic efficacy of magnesium chloride and ethyl alcohol in temperate octopus and cuttlefish species. *J. Am. Assoc. Lab. Anim. Sci.* **60**(5), 556–567 (2021).
23. DiBona, C. W., Williams, T. L., Dinneen, S. R., Jones Labadie, S. F. & Deravi, L. F. A method for extracting pigments from squid *Doryteuthis pealeii*. *J Vis Exp* (117). (2016).
24. Deerinck, T. J. et al. Enhancing serial block-face scanning electron microscopy to enable high resolution 3-D nanohistology of cells and tissues. *Microsc. Microanal.* **16**(S2), 1138–1139 (2010).
25. Sun, J., Bhushan, B. & Tong, J. Structural coloration in nature. *RSC Adv.* **3**(35) (2013).
26. Parker, A. R. 515 million years of structural colour. *J. Opt. A: Pure Appl. Opt.* **2**, R15 (2000).
27. Maia, R., Caetano, J. V., Bao, S. N. & Macedo, R. H. Iridescent structural colour production in male blue-black grassquit feather barbules: the role of keratin and melanin. *J. R Soc. Interface.* **6**(Suppl 2), S203–S211 (2009).
28. Jeon, D. J., Paik, S., Ji, S. & Yeo, J. S. Melanin-based structural coloration of birds and its biomimetic applications. *Appl. Microsc.* **51**(1), 14 (2021).
29. Teyssier, J., Saenko, S. V., van der Marel, D. & Milinkovitch, M. C. Photonic crystals cause active colour change in chameleons. *Nat. Commun.* **6**, 6368 (2015).
30. I Morehouse, N., Vukusic, P. & Rutowski, R. Pterin pigment granules are responsible for both broadband light scattering and wavelength selective absorption in the wing scales of pierid butterflies. *Proc. Royal Soc. B: Biol. Sci.* **274**(1608), 359–366 (2007).
31. Wilts, B. D., Wijnen, B., Leertouwer, H. L., Steiner, U. & Stavenga, D. G. Extreme refractive index wing scale beads containing dense pterin pigments cause the bright colors of pierid butterflies. *Adv. Opt. Mater.* **5**(3), 1600879 (2017).
32. Henze, M. J., Lind, O., Wilts, B. D. & Kelber, A. Pterin-pigmented nanospheres create the colours of the polymorphic damselfly *Ischnura elegans*. *J. R Soc. Interface.* **16**(153), 20180785 (2019).
33. Shavit, K. et al. A tunable reflector enabling crustaceans to see but not be seen. *Science* **379**, 695–700 (2023).
34. Futahashi, R., Kurita, R., Mano, H. & Fukatsu, T. Redox alters yellow dragonflies into red. *Proc. Natl. Acad. Sci.* **109**(31), 12626–12631 (2012).
35. Williams, T. L. et al. Contributions of phenoxazone-based pigments to the structure and function of nanostructured granules in squid chromatophores. *Langmuir* **32**(15), 3754–3759 (2016).
36. Kumar, A., Williams, T. L., Martin, C. A., Figueroa-Navedo, A. M. & Deravi, L. F. Xanthommatin-based electrochromic displays inspired by nature. *ACS Appl. Mater. Interfaces.* **10**(49), 43177–43183 (2018).
37. Kumar, A. et al. Natural light-scattering nanoparticles enable visible through short-wave infrared color modulation. *Adv. Opt. Mater.* **6**, 8 (2018).
38. Elofsson, R. & Hallberg, E. Correlation of ultrastructure and chemical composition crustracean chromatophore pigment. *J. Ultrastructure Res.* **44**, 421–429 (1973).
39. Sawada, H., Nakagoshi, M., Mase, K. & Yamamoto, T. Occurrence of xanthommatin containing pigment granules in the central nervous system of the silkworm, *Bombyx mori*. *Comp. Biochem. Physiol. Part. B.* **125**, 421–428 (2000).
40. Sawada, H., Tsusue, M., Yamamoto, T. & Sakurai, S. Occurrence of xanthommatin containing pigment granules in the epidermal cells of the silkworm, *Bombyx mori*. *Insect Biochem.* **20**(8), 785–792 (1990).
41. Shoup, J. R. The development of pigment granules in the eyes of wild type and mutant *Drosophila melanogaster*. *J. Cell. Biol.* **29**, 223–249 (1966).
42. Veron, J. E. N., O'Farrell, A. F. & Dixon, B. The fine structure of odonata chromatophores. *Tissue Cell.* **6**, 613–626 (1974).
43. Insausti, T. C. & Casas, J. The functional morphology of color changing in a spider: development of ommochrome pigment granules. *J. Exp. Biol.* **211**(Pt 5), 780–789 (2008).
44. Insausti, T. C. & Casas, J. Turnover of pigment granules: cyclic catabolism and anabolism of ommochromes within epidermal cells. *Tissue Cell.* **41**(6), 421–429 (2009).

45. D'Alba, L. & Shawkey, M. D. Melanosomes: biogenesis, properties, and evolution of an ancient organelle. *Physiol. Rev.* **99**(1), 1–19 (2019).
46. Eliason, C. M., Bitton, P. P. & Shawkey, M. D. How hollow melanosomes affect iridescent colour production in birds. *Proc. R. Soc. B Biol. Sci.* **280**(1767), 20131505. (2013).
47. Berger, C. et al. Plasma FIB milling for the determination of structures in situ. *Nat. Commun.* **14** (2023).
48. Sullivan, P. A., Wilson, D. J., Vallon, M., Bower, D. Q. & Deravi, L. F. Inkjet printing bio-inspired electrochromic pixels. *Adv. Mater. Interfaces* (2023).

Acknowledgements

The authors would like to acknowledge support from the Air Force Office of Scientific Research (FA9550-22-1-0467 to RTH, SLS and LFD). LFD and DQB would also like to acknowledge partial support from NSF DMR-1945207 and the Northeastern University Albert Sebag PhD `02 Graduate Fellowship. RTH acknowledges partial support from the Sholley Foundation and the Ben-Veniste Family Foundation.The authors thank Lydia Måthger for help with reflection optics for Fig. 1e, f. James Peyla was instrumental in obtaining correlated light and SEM images in Fig. 2. We thank Kyle Fisk for TEMs in Fig. 3c, and George Bell for Hollande's material for Fig. 3b. Special thanks to Alan Kuzirian (Hanlon Lab, MBL) for tissue preparation, and Lee Pullan and Vanessa Mazuzan (FEI, Thermo Fisher Scientific) and Stuart Searle (Gatan, Inc, and ConnectomX, Inc) for the SBFI image acquisitions.

Author contributions

D. Q. B. and S. L. S. wrote the main manuscript text and prepared all figures. Data collection and analysis was performed by S. L. S. and D. Q. B. All authors reviewed and edited the manuscript.

Declarations

Competing interests

The authors declare no competing interests.

Additional information

Correspondence and requests for materials should be addressed to L.F.D.

Reprints and permissions information is available at www.nature.com/reprints.

Publisher's note Springer Nature remains neutral with regard to jurisdictional claims in published maps and institutional affiliations.